

The Reconstruction and Calibration of the BESIII Main Drift Chamber

Zhang Yao, Liu Qiuguang, Wang Jike, Wu Linghui

Experimental Physics Center, 19B Yu Quan Road, Shijingshan District, Beijing 100049,
People's Republic of China

E-mail: zhangyao@mail.ihep.ac.cn

Abstract. The BESIII[1] detector designed for the upgrading Beijing Electron Positron Collider II(BEPCII)[2] will be commissioned at the summer of 2008. The Main Drift Chamber(MDC), which is most important sub-detector of the BESIII, is expected to provide good momentum resolution ($0.5\% @ 1\text{GeV}/c$) and tracking efficiency in a range of $0.5 \sim 2.0$ GeV/c . This makes stringent demands on the performance of the offline software. The event reconstruction and offline calibration algorithms have been developed using C++ language and object-oriented techniques under BESIII Offline Software System (BOSS)[3].

The reconstruction system consists of tracking and track fitting. Two tracking algorithms have been developed for MDC. One uses a template matching method to find track segments and combined them into track candidates followed by a least square fit, the other uses TSF method to find track segment. The track fitting based on Kalman filter method is used to handle the effects of material and non-uniform magnetic field. The implementation of the track finding, fitting algorithms and the performance with Monte Carlo data are presented.

The study of the offline calibration method using the cosmic ray data, including the calibration of the time-to-distance relation and the software alignment, also be presented.

1. Introduction

BESIII is a high precision detector in the e^+e^- collider for BEPCII running at the tau-charm energy region. The Main Drift Chamber (MDC) of BESIII is expected to provide particle momentum measurement, charged particle trigger at level one and the particle identification through dE/dx measurements. Track reconstruction and calibration in MDC will be a challenging task due to the high precise measurement and high luminosity. Efficient reconstruction with accurate track parameters is required in a wide range of momentum.

2. MDC Tracking

The two tracking algorithms, MdcPatRec[4] and TrkReco[5], are developed for the Main Drift Chamber of the BESIII detector using C++ language and object-oriented techniques under the BOSS framework. MdcPatRec is developed based on BaBar drift chamber tracking algorithm and TrkReco based on tracking algorithm used in Belle experiment, where least square method is used for track fitting in both algorithms.

2.1. Segment Finding With Template Matching Method in MdcPatRec algorithm

MdcPatRec searches for the segment in every super-layer through template matching method. First the segment finding algorithm searches the reference wires and their neighbor hits to form a hits-group as shown in Figure 1. The cell arrangement of BESIII is not symmetric (90-degree symmetrical in inner chamber and stepped region, 22.5-degree symmetrical in outer chamber). To solve this problem, take 2 reference wires and their azimuthal angle are used to calculate cell index of “neighbor” wires.

The dictionary of MdcPatRec contains 8 templates with 4 hits and 20 templates with 3 hits as shown in Figure 2. The successful matching hits-group will be stored as segment which will be fitted to get the segment parameters.

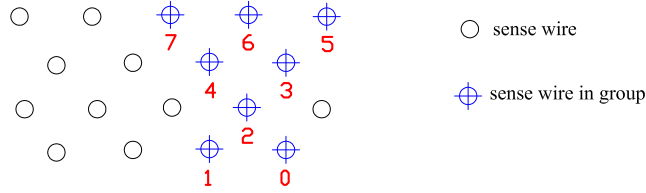


Figure 1. Neighbor wires of one super-layers in hits-group

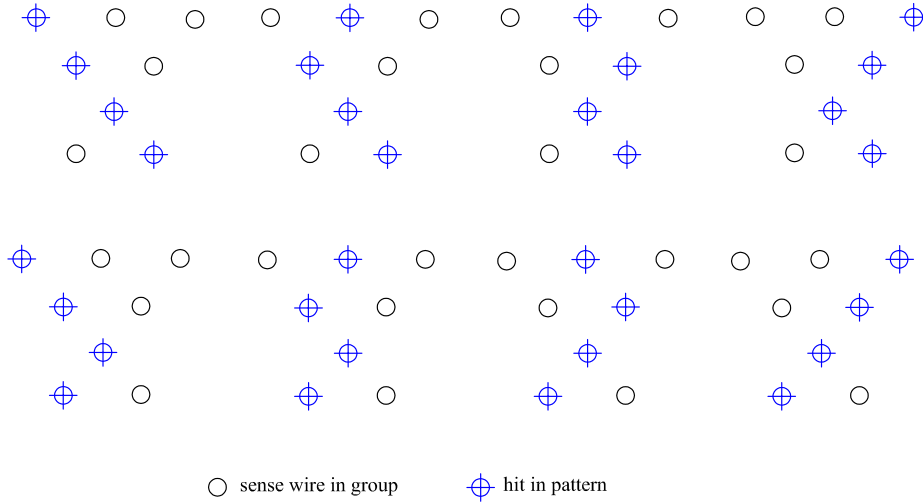


Figure 2. 4-hits-group in patten dictionary

2.2. Segment Finding Using TSF Method in TrkReco algorithm

In conformal transformation, a hit position (x, y) in the $x-y$ plane is transformed into a position (X, Y) in the conformal plane as,

$$X = \frac{2x}{x^2 + y^2}, \quad Y = \frac{2y}{x^2 + y^2}. \quad (1)$$

Through the conformal transformation, a circle which passes through the origin $(0,0)$ is transformed into a line. Typically, a valid segment pattern consists of hits contiguous in space and time. The *drift circle*¹ of valid hit for a given track is tangent to the line of the track in

¹ represent the hit wires; a circle has its wire position as the center and its drift distance as the radius.

conformal plane. If a hit does not belong to this track, its drift circle in the conformal plane would not necessarily be tangent to the line of this track. This unique feature can be used to reject background hits at the track finding stage, as described below.

There are 4 layers within one super-layer. To allow inefficiency of a given layer, 3 out of 4 layers are required to have hits for a given track segment within a super-layer. The track segment finding thus can start either from a cell at the inner most layer (layer 0) or the second layer (layer 1) next to it in case the inner layer does not have a hit due to inefficiency. Therefore, there are two combinations: 4 out of 4 and 3 out of 4. There are two possible groups or combinations of cell as shown in Figure 3 a). Figure 3 b) shows the group in the conformal plane where the range of the area is represented by two the dashed-lines. The TSF algorithm starts from the inner most hit first, with a line fitted for each outer layer hit circle to the inner layer hit circle in the conformal plane, resulting in multiple potential lines as shown in Figure 3 c). To determine which line represents the valid track segment, the hit information from the two middle layers are then used. The lines tangent to the *drift circles* in the two middle layers are the potential line for a track. Figure 3 d) shows a valid track segment found using this method.

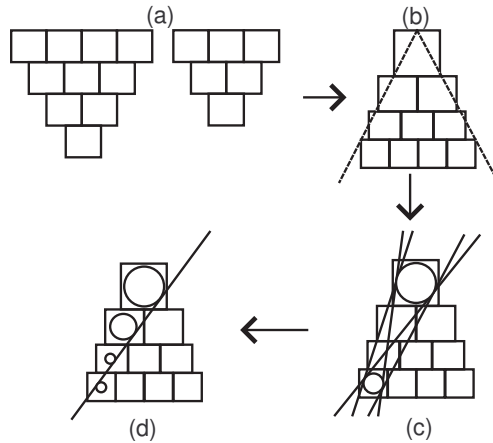


Figure 3. a) Two original types of TSF model are defined. b) Four-layer type pattern in conformal plane. c) Four lines are fitted out by the *drift circles* of the inner and outer hits. d) With the other hits in this model, whose *drift circle* can be appended on these lines in some conditions, a track segment is constructed.

As will be shown later, the TSF method described above not only makes the algorithm more robust against high random background hits in the chamber due to beam related background or electronics noises, but also makes it less sensitive to low p_t tracks curving within the chamber producing multiple circles of hits along the z direction (the so called curlers). This is because the drift circles from the later stage of the curler are no longer tangent to the original track in the conformal plane, due to energy loss etc. Therefore, those hits are unlikely causing confusion to the reconstruction of the original track (thus not affecting the tracking efficiency), although redundant or more tracks could be reconstructed from them due to the nature of the curler.

2.3. Performance of Tracking

2.3.1. Efficiency The track efficiency versus transverse momentum is shown in Figure 4, using the TSF method. The efficiency is still high even for p_t as low as $0.06 \text{ GeV}/c$. This is good because $0.05 \text{ GeV}/c$ is the minimum p_t at which charged tracks can only travel 2 stereo super-layers and 1 axial super-layer. Note that the efficiency of the TSF method exceeds 100% in the p_t range

below $0.12\text{GeV}/c$, this is due to the fact that tracks curling up in MDC could be reconstructed redundantly (note that the redundant tracks can be removed at a later stage, which will be described elsewhere).

Figure 5 shows the effect of background noise level on the tracking efficiency using the TSF method. Clearly, the TSF-based tracking algorithm is robust against the background noise level, with the efficiency still better than 95% when the noise level reaches as high as 60%.

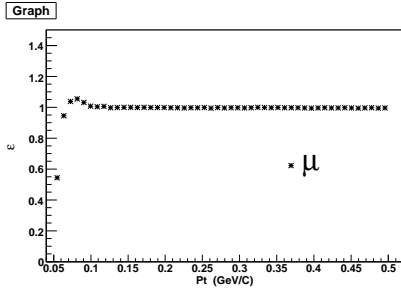


Figure 4. Efficiencies depend on transverse momentum for single μ .

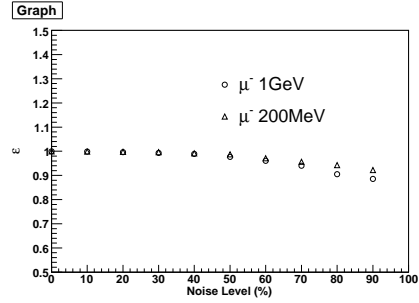


Figure 5. Efficiency distribution on different noise level.

2.3.2. Momentum and Spatial Resolution The momentum resolution is mainly infected by the position resolution and multiple scattering. In BESIII, the design goal is:

$$\sigma_{p_t}/p_t = (0.32\%p_t) \oplus (0.37\%/\beta). \quad (2)$$

The first term on the right-hand side is the effect of position resolution, the second term is the effect of multiple scattering. Figure 6 indicates the momentum resolution in reconstruction are better than expectation when the p_t is larger than $0.3\text{GeV}/c$.

Spatial resolution is represented by the resolution of residual, where residual measured by comparing the drift distance and the distance of closest approach to fitted track. Figure 7 shows the distribution of residual and the average spatial resolution of all layers is $126\mu\text{m}$, which is comparable to the $120\mu\text{m}$ of Monte Carlo input.

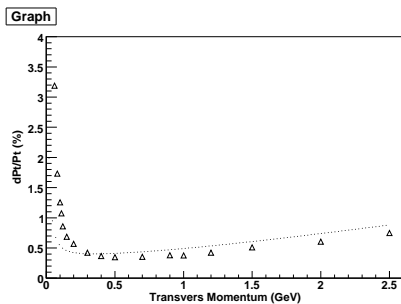


Figure 6. The transverse momentum resolution distribution of single μ event on different p_t , in which the dashed line is the expected momentum resolution for μ .

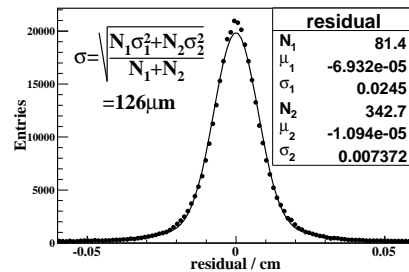


Figure 7. Residual distribution of $J/\psi \rightarrow \mu^+ \mu^-$ event.

2.3.3. *Physics Performance* Physics performance check is enhanced by Monte Carlo $\psi(2S) \rightarrow \pi^+\pi^-J/\psi, J/\psi \rightarrow \mu^+\mu^-$ channel with the final states of $\pi^+\pi^-\mu^+\mu^-$. According to the kinetic characteristics in this process, an obvious resonance of J/ψ can be seen in the recoil mass of $\pi^+\pi^-$ the invariant mass of $\mu^+\mu^-$. The reconstructed momentum of $\pi^+\pi^-$ and $\mu^+\mu^-$ are used in calculation, so we can use this channel to analyze the momentum resolution of reconstruction in drift chamber. The recoil and invariant mass distributions are shown in Figure 8 and Figure 9 which the resolution is defined with $\sigma = f\sigma_1 + (1-f)\sigma_2$. The recoil and invariant mass resolution about 3.0 MeV, 16.6 MeV respectively with TrkReco algorithm and 3.3 MeV, 13.6 MeV with MdcPatRec algorithm. They are consistent with each other.

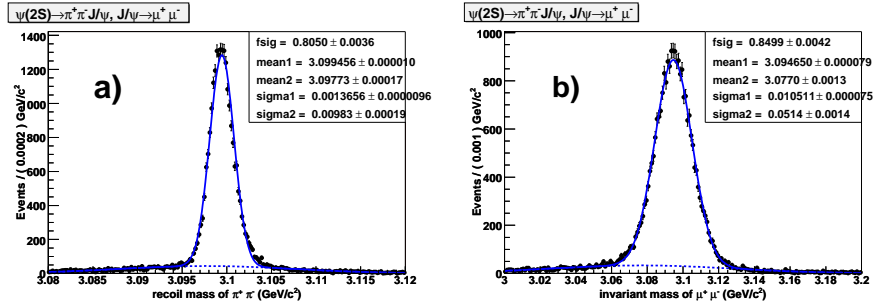


Figure 8. Recoil mass (a) and invariant mass (b) of $\psi(2S) \rightarrow \pi^+\pi^-J/\psi \rightarrow \pi^+\pi^-\mu^+\mu^-$ event by TrkReco.

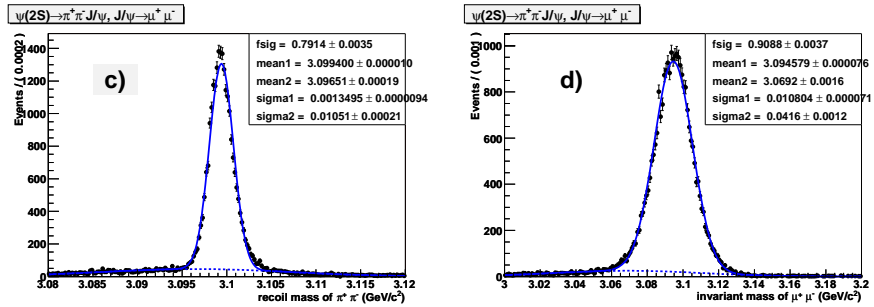


Figure 9. Recoil mass (c) and invariant mass (d) of $\psi(2S) \rightarrow \pi^+\pi^-J/\psi \rightarrow \pi^+\pi^-\mu^+\mu^-$ event by MdcPatRec.

3. Mdc Track Fitting

In the MDC tracking stage, in order to save time and other reason, the track material effects and NUMF is ignored. So more precise correct is done in track fitting using Kalman filter method[6]. This method updates fitting results in each step and easy to deal with material effects and magnetic filed distortions to yield more accurate track parameters and error matrix. A complete Kalman filter include three processes:

- **Predication** Estimation of state vector at future time $k+1$ with information at k .
- **Filtering** Update the state vector by taking now measurement into consideration.
- **Smothering** Backward estimation of state vector at k with all measurement $n(n>k)$

3.1. Handling material effects

When a charged particle traverses through matter, the main interaction are energy loss and multiple scattering. In BESIII situation, for path of length l , the contribution of multiple scattering to the error matrix is:

$$V_{ms} = \Theta_0^2 \begin{pmatrix} l^2/3 & (p/p_t)l/2 & 0 & 0 & 0 \\ (p/p_t)l/2 & (p/p_t)^2 & 0 & 0 & 0 \\ 0 & 0 & (\kappa \tan \lambda)^2 & (p_z/p)\kappa l/2 & (p/p_t)^2 \kappa \tan \lambda \\ 0 & 0 & (p_z/p)\kappa l/2 & (p_t/p)^2 l^2/3 & (p/p_t)l/2 \\ 0 & 0 & (p/p_t)^2 \kappa \tan \lambda & (p/p_t)l/2 & (p/p_t)^4 \end{pmatrix} \quad (3)$$

Also, due to ionization and radiation, the particle will lose some energy when it get through matter, which may affect trajectory. We calculate it by the standard Bethe-Bloch formula:

$$\Delta p = \int_0^t \frac{dp}{dx} dx = \int_0^t \frac{1}{\beta} \frac{dE}{dx} dx = \int_0^t \frac{A}{\beta^3} \left[\ln \left(\frac{2m_e c^2 \beta^2 \gamma^2}{I_0} \right) - \beta^2 \right] dx \quad (4)$$

3.2. Handling non-uniform magnetic filed effect(NUMF)

In the Kalman fitting algorithm, the track parameters are transported with nominal magnetic field and handle the NUMF as perturbation. The initial track is divided into many segments, the more non-uniform, the smaller the segment is. In each step, the modification to momentum due to NUMF can be expressed as path integral:

$$\vec{\Delta p} = \int_{l_0}^{l_1} (\vec{B} - \vec{B}_{nom}) \times \vec{dl} \quad (5)$$

Through this formula, we can calculate out the change of the track parameters caused by the momentum as following:

$$\Delta \phi_0 = |\kappa| (\Delta p_y \cos \phi_0 - \Delta p_x \sin \phi_0) \quad (6)$$

$$\Delta \kappa = |\kappa| \kappa (\Delta p_x \cos \phi_0 + \Delta p_y \sin \phi_0) \quad (7)$$

$$\Delta \tan \lambda = \Delta p_z |\kappa| + \frac{\tan \lambda \Delta \kappa}{\kappa} \quad (8)$$

3.3. Performance of KalFitAlg algorithm

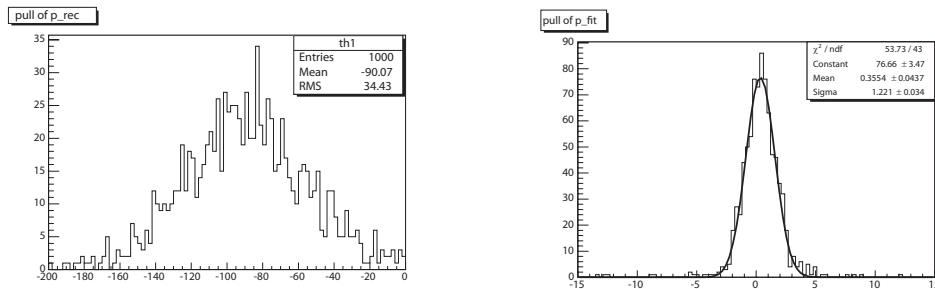


Figure 10. Pull momentum distribution of single μ at $0.3\text{GeV}/c$ before(left) and after(right) Kalman fitting.

After the precise corrections of Kalman filter fitting, the track parameters are improved very well as shown in Figure10.

4. Mdc Calibration and Alignment

To achieve accurate measurements, a precise offline calibration, including the calibration of the time-to-distance relation, T0 etc, are required. The time-to-distance relation is fitted to a 5th order polynomial plus 1st order polynomial near the edge of the cell as shown in Figure 11 and determined layer by layer. T0 is determined cell by cell based on the residual distribution. The calibration software for the drift chamber, MdcCalibAlg, has been developed. A preliminary test with Monte Carlo simulation has been finished. The software runs well and the results are well converged.

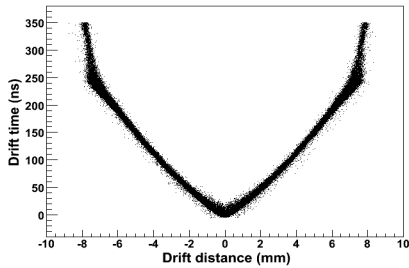


Figure 11. Drift time-to-distance relation

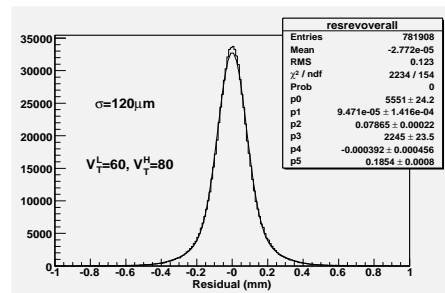


Figure 12. Residual of the outer chamber axial layers

In addition, a software alignment is necessary to reduce the effect of mechanical imperfection on the reconstruction. We have investigated three alignment methods: Millepede matrix method, Kalman filter method and residual distribution method. The application of three methods to the MDC has been studied with Monte Carlo simulation. The result shows that these methods are effective in the estimation of alignment parameters.

A cosmic ray test without magnetic field has been carried out to inspect the quality of the chamber and to commissioning the chamber with other sub-systems of BESIII. Preliminary results show that the drift chamber system is working normally. Figure 12 shows that the resolution of residual of the outer chamber axial layer is $120\mu\text{m}$. Study of the calibration and alignment using data of the cosmic ray test is in process.

References

- [1] Preliminary Design Report of the BES III detector, Jan, (2004)
- [2] BEPCII Preliminary Design Report, (2002)
- [3] LI Wei-Dong, LIU Huai-Min et al. The Offline Software for the BESII Experiment. Proceeding of CHEP06. Mumbai, 2006
- [4] ZHANG Yao et al. The Design and Implementation of MdcPatRec Tracking Algorithm for the BESIII Main Drift Chamber, 27(2007) 665-669 (in Chinese)
- [5] LIU Qiu-Guang et al. Track Reconstruction Using the TSF Method for the BESIII Main Drift Chamber, High Energy Physics and Nuclear Physics, to be published
- [6] WANG Da-Yong et al. Kalman Track Fitting for BESIII. Nuclear Electronics and Detection Technology, 27(2007) 658-664 (in Chinese)